AIAA 80-0139R

Numerical Solutions of a Reduced pdf Model for Turbulent Diffusion Flames

R. J. Bywater*
The Aerospace Corporation, El Segundo, Calif.

Solutions are presented for the turbulent diffusion flame in a two-dimensional shear layer based upon a kinetic theory of turbulence (KTT). The fuel and oxidizer comprising the two streams are considered to react infinitely fast according to a one-step, irreversible kinetic mechanism. The solutions are obtained by direct numerical calculation of the transverse velocity probability density function (pdf) and the associated species distributions. The mean reactant profiles calculated from the solutions display the characteristic thick, turbulent flame zone. The phenomena result from the fact that, in the context of the KTT, species react only when in the same velocity cell. This fact coincides with the known physical requirement that molecular mixing precede reaction. The solutions demonstrate this behavior by showing how reactants can coexist in the mean, even when infinite reaction rates are enforced at each point $(t,\tilde{x},\tilde{u})$ of velocity space.

Introduction

GREAT interest is shown in pdf models[1,2] of turbulence and particularly in those of reacting turbulent flows. This is due to the inability of previous phenomenological theories, based upon Prandtl's original ideas, to account even qualitatively for the fundamental turbulent diffusion flame structure. Further inability to perform accurate engineering predictions of flowfield phenomena for such applications as turbulent combustion, rocket plumes, and chemical lasers has resulted in attempts, via pdf's, to investigate the underlying statistical structure of velocity and scalar averages required for engineering analyses. This paper presents current results of a continuing effort to describe the significant engineering aspects of turbulent flowfields using one of the first pdf models to be developed for that purpose by Chung.[3]

Previous investigations[4-6] based upon the present model have focused primarily upon the ability of such a kinetic theory of turbulence (KTT) to explain the observed features of turbulent flows, such as the thick, turbulent diffusion flame in the limit of fast reactions. The tool employed was the Liu-Lees[7] moment method of approximation, which was used to determine the mean flowfield structure. The success of that work suggests the value of exploring further applications of the KTT. The purpose of the present work is to develop direct numerical solutions for the pdf upon which the KTT is based. In doing so, a better understanding of turbulent structure is gained through the more detailed velocity space description, which was not accessible in previous studies. In addition, the numerical solutions open the way for investigation of more complex engineering geometries than the one-dimensional geometries that provided the test beds for establishing the basic turbulence phenomena.

Reference 8 was the initial step in performing numerical calculations for the velocity pdf of the present theory. In that work, solutions were obtained for the transverse turbulence field of an inert, incompressible, two-dimensional free shear layer. The same geometry is employed in Fig. 1, where one stream contains an oxidizer plus a diluent and the other contains a fuel. As the two streams mix, a turbulent diffusion flame is established. The effects of the combustion on the velocity field through compressibility are neglected. Therefore, the calculated velocity field is the same as that obtained in Ref. 8. The new results contained in this paper are the species distributions in velocity space which constitute the diffusion flame in the limit of infinite reaction rates. Because the present model is based upon the velocity pdf, intimate coupling between the mixing and reaction phenomena is inherent in the solutions. Investigation of these solutions in the following sections will reveal that the distinguishing nature of the turbulent diffusion flame can be understood by viewing the result of enforcing fast-reaction kinetics at each location $(t,\tilde{x},\tilde{u})$ of phase space.

Presented as Paper 80-0139 at the AIAA 18th Aerospace Sciences Meeting, Pasadena, Calif., Jan. 14-16, 1980; submitted Aug. 12, 1980; revision received Sept. 28, 1981.

*Engineering Specialist, Fluid Mechanics Department. Member AIAA.

Formulation

Governing Equations

The KTT,[6] which forms the basis for the present study, uses a pdf, $f(t,\tilde{x},\tilde{u})$, to describe the turbulence velocity field. Because this theory was developed primarily to increase understanding of mixing coupled reacting flows, the species description is tied directly to the velocity field and hence to the mixing phenomena. The following expressions relate the kinetic theory description to the mean quantities of engineering interest, where the averaging process is defined as

$$\langle Q(\tilde{u})\rangle = \int_{-\infty}^{\infty} Q(\tilde{u}) f(t,\tilde{x},\tilde{u})\,d\tilde{u}$$

with the familiar scalar and velocity moments resulting from specific Q-functions

$$\langle u_i\rangle = \int_{-\infty}^{\infty} u_i f\,d\tilde{u} \equiv \text{mean velocity } (u_{0i}) \tag{1}$$

$$U_i = u_i - \langle u_i\rangle \equiv \text{relative velocity}$$

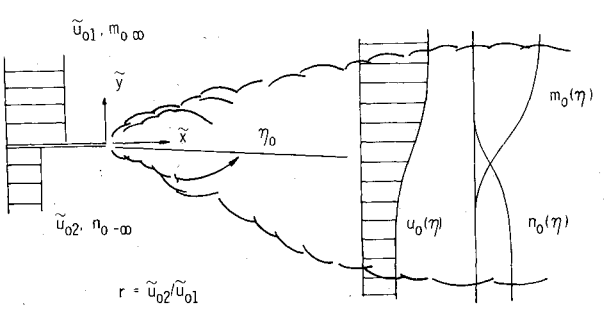

Fig. 1 Turbulent diffusion flame in a two-dimensional shear layer.

$$\langle z_\ell \rangle = \int_{-\infty}^{\infty} F_\ell(t,\bar{x},\bar{u})\,d\bar{u} \equiv \text{mean mass fraction of species } \ell$$

$$\langle z_\ell U_i \rangle = \int_{-\infty}^{\infty} U_i F_\ell(t,\bar{x},\bar{u})\,d\bar{u} \equiv \text{turbulent transport of species } \ell$$

The F_ℓ associates a value z_ℓ of the ℓ-species mass fraction with a fluid element whose velocity is in the range $\bar{u}$ to $\bar{u}+d\bar{u}$ at time t and position $\bar{x}$. This description of the species distribution generalizes the molecular kinetic theory treatment of number density. This approach differs from that of treating the pdf for the chemical species, in which the species mass fraction is itself an independent variable. A discussion of the relationship between the two representations of turbulent reacting flows is given by Chung.[6]

One distinction noted herein is apparent when the pdf for the chemical species is employed in a model[9] defined as follows:

$$P_\ell(t,\bar{x},z_\ell) = \int_{-\infty}^{\infty} P(t,\bar{x},z_\ell,\bar{u})\,d\bar{u} \tag{2}$$

where P is the one point joint pdf for the velocity and species fields at time t and position $\bar{x}$. When the governing equation for P_ℓ is derived, terms arise representing the coupling with the velocity field, which must be modeled in much the same way as the transport terms $\langle z_\ell \bar{u} \rangle$, which arise in the mean species conservation equations. The kinetic theory approach used herein requires no modeling of transport processes because $F_\ell(t,\bar{x},\bar{u})$ is a function of the velocity field. The coupling between the velocity field and the chemical processes, which is the distinguishing feature of turbulent diffusion flames, is an integral part of the solution for F_ℓ. The solutions obtained and presented in this paper make it possible to explore this behavior by virtue of the velocity space dependence.

Details of the derivation of the governing equations for f and F_ℓ can be found elsewhere,[10] with only the results presented here:

$$u_j \frac{\partial f}{\partial x_j} = \beta\left[(1+D)\frac{\partial}{\partial U_j}(U_j f) + \frac{\langle U_k U_k \rangle}{3}\frac{\partial^2 f}{\partial U_j \partial U_j}\right] \tag{3}$$

$$u_j \frac{\partial F_\ell}{\partial x_j} = \beta\left[(1+D)\frac{\partial}{\partial U_j}(U_j F_\ell) + \frac{\langle U_k U_k \rangle}{3}\frac{\partial^2 F_\ell}{\partial U_j \partial U_j}\right] - \beta D(F_\ell - f\langle z_\ell \rangle) + W_\ell f \tag{4}$$

Subscripts j and k are tensor indices, with repeated indices indicating summation. Symbols x_j, u_j, and U_j represent, respectively, the jth components of the position vector $\bar{x}$, instantaneous velocity vector $\bar{u}$, and relative velocity vector $\bar{U}$. $\langle z_\ell \rangle$ is the average mass fraction of the ℓth species, and D is the ratio of the turbulent dissipation rate to the equilibration rate β of the large eddies responsible for the observed characteristics of high Reynolds number flows. The symbol β is defined as

$$\beta = A\langle U_k U_k \rangle^{1/2}/2\Lambda \tag{5}$$

where, in previous studies,[6] A was constrained to be of order 1. The W_ℓ is the chemical production rate of the species ℓ per unit mass of the fluid.

Equilibrium Turbulent Combustion

For the present problem, Fig. 1 illustrates the flowfield geometry. It consists of two parallel turbulent streams of mean velocities u_{01} and u_{02}. One stream carries a fuel, while the other carries an oxidizer plus a diluent. The oxidizer and fuel react according to the following one-step combustion reaction:

$$a(\text{fuel}) + b(\text{oxidant}) \xrightarrow{k_f} d(\text{product}) \tag{6}$$

where a, b, and d represent the number of moles of each species. The instantaneous production rate of combustion products is given by

$$W_p = K\exp[-(\Delta E/R)(T^{-1} - T^{*-1})]z_r^a z_s^b \tag{7}$$

$$K = k_0(d\hat{M}_p/\hat{M}_r^a \hat{M}_s^b)\rho^{a+b-1}\exp(-\Delta E/RT^*) \tag{8}$$

where k_0 is a constant and ΔE and R are the activation energy and the gas constant, respectively; T is the instantaneous absolute temperature. The $(\,)^*$ represents a mean value associated with chemical equilibrium at the edge of the flame. The subscripts r, s, and p refer to fuel, oxidant, and products, respectively. The $\hat{M}$ is the molecular weight, and ρ is the gas density. The instantaneous production rates of fuel W_r, oxidant W_s, and energy W_t due to chemical reactions are related to W_p.

The full set of equations is represented by Eq. (4) with

$$\ell = \begin{cases} r \\ s \\ p \\ t \quad (z_t \equiv T) \\ c - \text{inert species, } W_c \equiv 0 \end{cases}$$

The reaction terms can be eliminated in all but the equation for t with the transformation

$$F_m = (d\hat{M}_p/a\hat{M}_r)F_r, \quad F_n = (d\hat{M}_p/b\hat{M}_s)F_s$$

$$F_h = (C_p/\Delta h^0)F_t, \quad F_\alpha = F_m + F_h, \quad F_\gamma = F_n + F_h \tag{9}$$

where Δh^0 and C_p are the heat of reaction and specific heat, respectively. The result is the following equations for F_α, F_γ, and F_h:

$$u_j \frac{\partial F_h}{\partial x_j} = \beta\left[(1+D)\frac{\partial(U_j F_h)}{\partial U_j} + \frac{\langle U_k U_k \rangle}{3}\frac{\partial^2 F_h}{\partial U_j \partial U_j}\right] - \beta D(F_h - h_0 f) + W_p f \tag{10}$$

$$u_j \frac{\partial F_\alpha}{\partial x_j} = \beta\left[(1+D)\frac{\partial(U_j F_\alpha)}{\partial U_j} + \frac{\langle U_k U_k \rangle}{3}\frac{\partial^2 F_\alpha}{\partial U_j \partial U_j}\right] - \beta D(F_\alpha - \alpha_0 f) \tag{11}$$

$$u_j \frac{\partial F_\gamma}{\partial x_j} = \beta\left[(1+D)\frac{\partial(U_j F_\gamma)}{\partial U_j} + \frac{\langle U_k U_k \rangle}{3}\frac{\partial^2 F_\gamma}{\partial U_j \partial U_j}\right] - \beta D(F_\gamma - \gamma_0 f) \tag{12}$$

The symbols h_0, α_0, and γ_0 represent the mean values of h, α, and γ, respectively. Equations (3), (10-12), and (4) (with $\ell = c$) as well as the auxiliary relationships (7-9) govern the mixing and combustion of reactants in the two-stream mixing layer of Fig. 1. Manipulation of the governing equations has resulted in the chemical source terms being limited to the equation for F_h. The solution for the combustion products is obtained by noting that the mass fractions for all species must sum to 1.

The present work is concerned with the case in which $K \to \infty$, establishing equilibrium combustion within the shear layer. Application of this limit to Eq. (10) has been shown[6] to result in the following algebraic equation:

$$F_m F_n = 0 \tag{13}$$

Equation (13) replaces Eq. (10) in the set of governing equations. This condition appears analogous to that imposed upon reactant concentrations in laminar flame sheet analyses.[11] One important difference is that F_m and F_n are functions of the independent velocity variable.

The coupling between the scalar and velocity fields inherent in the present model and emphasized in Eq. (13) is at the root of the turbulent diffusion flame structure. This equation states that, for an infinitely fast combustion reaction, the fuel and oxidizer cannot coexist in the same velocity cell. The fact that Eq. (13) is satisfied at each point of velocity space implies that reactions cannot proceed until the reactants enter the same velocity cell. Under the present restriction of infinite reaction rates, they are then immediately consumed. Therefore, the ability of the reactants to react depends upon their history in the turbulence field. This behavior of the present statistical model parallels the commonly accepted physical explanation for such turbulent chemical coupling phenomena as the thick, turbulent diffusion flame. That is, chemical processes are molecular and thus require mixing at the molecular level before reactions proceed. Turbulent mixing, on the other hand, is a gross phenomenon in which molecular mixing may not be completed to the degree indicated by mean profiles that give the appearance of coexisting reactants even at infinite reaction rates. The physical explanation for this phenomenon is that the turbulent eddies must break down and interdiffuse to allow molecular reactions to proceed. This is synonymous with the present description, which requires the reactants to occupy the same cell in phase space before they can react. The advantage of the present velocity description in clarifying this aspect of the physics will be apparent when the solutions are discussed.

Before discussing the solution of the governing equations, they will first be put in a form appropriate to the present geometry by transforming them to shear layer coordinates and employing the reduction technique of Ref. 8.

Reduced Equations for f_V and $F_{V\ell}$

The structure of the turbulent diffusion flame that develops in a similar two-stream mixing layer is primarily determined by the turbulent transport in the transverse direction. Therefore, attention is focused upon this element of the turbulence field by treating the velocity and species distributions for the transverse component of the velocity only. This is accomplished by the following reduction:

$$f_{\tilde{V}}(t,\tilde{x},\tilde{V}) = \int_{-\infty}^{\infty}\int_{-\infty}^{\infty} f(t,\tilde{x},\tilde{U},\tilde{V},\tilde{W})\,\mathrm{d}\tilde{U}\mathrm{d}\tilde{W}$$

$$F_{\tilde{V}\ell}(t,\tilde{x},\tilde{V}) = \int_{-\infty}^{\infty}\int_{-\infty}^{\infty} F_\ell(t,\tilde{x},\tilde{U},\tilde{V},\tilde{W})\,\mathrm{d}\tilde{U}\mathrm{d}\tilde{W} \qquad (14)$$

where $(\tilde{x},\tilde{y},\tilde{z})$ and $(\tilde{U},\tilde{V},\tilde{W})$ represent the dimensional Cartesian components (x_1,x_2,x_3) and (U_1,U_2,U_3), respectively. The governing equations for $f_{\tilde{V}}$ and $F_{\tilde{V}\ell}$ are obtained from the equations for f and F_ℓ by integrating them over all $\tilde{U}$ and $\tilde{W}$. Details can be found in Ref. 8, which shows how a generalized moment equation can be developed by first multiplying the equation by some general function of the velocity field and then integrating over $\tilde{U}$ and $\tilde{W}$. The generalized reduction technique will be required for future investigations in which the complete turbulence field will be predicted. For the present work, however, only the lowest-order moment equation is needed to understand the important features of the diffusion flame while a significant simplification of the solution procedure is introduced. The resulting equations after transformation to shear layer coordinates $(x,y,V)\rightarrow(x,\eta,V)$ and nondimensionalization are written as

$$u_0 x\frac{\partial f_V}{\partial x} + V\frac{\partial f_V}{\partial \eta} = B\epsilon^{1/2}\left\{(1+D)\frac{\partial}{\partial V}[(V+u_0\eta-v_0)f_V] + \frac{\epsilon}{3}\frac{\partial^2 f_V}{\partial V^2}\right\} \qquad (15)$$

$$u_0 x\frac{\partial F_{V\ell}}{\partial x} + V\frac{\partial F_{V\ell}}{\partial \eta} = B\epsilon^{1/2}\left\{(1+D)\frac{\partial}{\partial V}[(V+u_0\eta-v_0)F_{V\ell}] + \frac{\epsilon}{3}\frac{\partial^2 F_{V\ell}}{\partial V^2}\right\} - BD\epsilon^{1/2}(F_{V\ell}-z_{\ell 0}f_V) \qquad (16)$$

where

$$\tilde{u}_0=\langle u_1\rangle \quad u_0=\tilde{u}_0/u_{01} \quad \epsilon=\sigma^2\langle U_kU_k\rangle/u_{01}^2$$
$$\tilde{v}_0=\langle u_2\rangle \quad v_0=\tilde{v}_0/u_{01} \quad \hat{V}=\sigma\tilde{V}/u_{01}$$
$$\ell=\alpha,\gamma,c \quad x=\tilde{x}/L \quad V=\hat{V}+v_0-u_0\eta$$
$$f_V=(u_{01}/\sigma)\tilde{f}_{\tilde{V}}$$
$$z_{\ell 0}=\left\{\begin{matrix}\alpha_0\\ \gamma_0\\ c_0\end{matrix}\right\} \quad \eta=\sigma\tilde{y}/\tilde{x} \quad F_{V\ell}=(u_{01}/\sigma)\tilde{F}_{\tilde{V}\ell} \qquad (17)$$

The symbols u_{01} and u_{02} represent the mean velocities of the high- and low-speed streams, respectively, with their ratio given by $r=u_{02}/u_{01}$. The transformed velocity coordinate V is introduced for computational convenience, while results will be presented in terms of $\hat{V}$. The scale length L is related to the virtual origin of the shear layer.[12]

Since only the transverse component of the distributions is being considered, certain mean flowfield information will be supplied, as was done in the previous study of Ref. 8. This represents no loss in generality, for it is possible to compute all the mean flow information that is to be used herein. This simply means the reduction technique is expanded to include additional reduced moment equations for the additional information. Doing so does not introduce the independent variables $(\tilde{U},\tilde{W})$ and therefore does not represent an increase in complexity beyond practicality.

The inputs are briefly summarized here. The integral length scale Λ was related[8] to the shear layer thickness as $\Lambda=\ell_s x$, resulting in the following expression for B:

$$B=A/2\sigma\ell_s \qquad (18)$$

where σ is the standard scaling parameter for the normal coordinate transformation and ℓ_s relates Λ to the shear layer thickness. As a result, B is a geometry-dependent constant.

The mean velocity and turbulence energy are given by[12,13]

$$u_0=(1+r/2)[1+(1-r/1+r)\mathrm{erf}(\eta-\eta_0)] \qquad (19)$$

$$\epsilon(\eta)=\epsilon_0\exp(-1.4\,|\eta-\eta_0|^{1.8}) \qquad (20)$$

where ϵ_0 is the value of ϵ on the dividing streamline η_0. The values of all the parameters in Eqs. (15-20) are the same as those used in Ref. 8 and correspond to the experimental conditions of Spencer and Jones[12] for $r=0.3, 0.6$.

When the infinite reaction kinetics are applied to the present solutions for the transverse velocity space description, it is assumed that, since this component of the turbulence field accounts for the major phenomena of interest, Eq. (13) can be

replaced by

$$F_{Vm}F_{Vn}=0 \tag{21}$$

The application of Eq. (21) in conjunction with the solutions for $F_{V\alpha}$ and $F_{V\gamma}$ to obtain the solutions for F_{Vm} and F_{Vn} is analogous to the procedure developed for laminar diffusion flames detailed in Ref. 11. This is accomplished by considering the difference $F_{Vm}-F_{Vn}$. The noncoexistence indicated by Eq. (21) means that this difference is equal to F_{Vm} when greater than zero and is equal to F_{Vn} when less than zero. When this manipulation is combined with the reduced form of the $(F_m, F_n, F_h)\rightarrow(F_\alpha, F_\gamma, F_h)$ transformation of Eq. (9), a direct relation between the $F_{V\alpha}$, $F_{V\gamma}$ and the F_{Vm}, F_{Vn} solutions is obtained.

Also, it is easier to observe the mechanics of turbulent diffusion flames with the present reduced description because three-dimensional plots of f_V and $F_{V\ell}$ vs η and V can readily be made. Higher-dimensional solutions cannot be viewed as easily.

The next section will address briefly the solution technique. Following that, the results will be presented and discussed.

Solution Procedure

Equations (15), (16), and (21), as well as the following equation, form the set for which solutions were obtained.

$$\langle z_p\rangle = 1-\langle z_c\rangle-\langle z_r\rangle-\langle z_s\rangle \tag{22}$$

Boundary conditions imposed upon f_V, $F_{V\alpha}$, $F_{V\gamma}$, and F_{Vc} are

$$\eta\rightarrow\infty,\quad V<0$$

$$f_V(\eta,V)\rightarrow f_G^+(V),\quad F_{V\ell}(\eta,V)\rightarrow z_{\ell 0}^+ f_G^+(V)$$

$$\eta\rightarrow-\infty,\quad V>0$$

$$f_V(\eta,V)\rightarrow f_G^-(V),\quad F_{V\ell}(\eta,V)\rightarrow z_{\ell 0}^- f_G^-(V)$$

$$V\rightarrow\pm\infty,\quad \text{all } \eta$$

$$f_V(\eta,V)\rightarrow 0,\quad F_{V\ell}(\eta,V)\rightarrow 0,\quad \ell=\alpha,\gamma,c \tag{23}$$

Boundary conditions on the reactant distributions at $\eta\rightarrow\pm\infty$ imply that all fluid elements in both streams have uniform concentrations. The only fluctuations that may exist in the oncoming streams are in velocity, as specified by $f_G^{\pm}$. These boundary conditions are summarized graphically in Fig. 2 along with the computational grid employed, where

$$f_G^{\pm}=\left(\frac{2\pi\epsilon^{\pm}}{3(1+D)}\right)^{-1/2}\exp\left[-\frac{(V-v_0+u_0\eta)^2}{(2\epsilon^{\pm}/3)(1+D)}\right] \tag{24}$$

and $\epsilon^{\pm}$ represents the nondimensional turbulence energy in the two streams $\eta\rightarrow\pm\infty$. The symbols $z_{\ell 0}^{\pm}$ represent the species mass fractions in the bounding streams.

The physical basis for the split-boundary conditions is the mechanism for turbulent ingestion into the shear layer. All turbulent excursions across the $\eta\rightarrow+\infty$ turbulent-nonturbulent interface associated with shear layer growth correspond to negative values of the fluctuating velocity field and bear the characteristics of the bounding uniform stream. This is analogous to the emission of molecules into a space from a bounding surface. Similarly, at $\eta\rightarrow-\infty$ only the fluid elements with positive velocities being drawn into the shear layer can be freely specified. The characteristics of the negative velocity fluctuations in that region are a result of calculation. As such, the split-boundary conditions are a natural result of the physics of the problem and provide a well-posed mathematical problem. Greater details are given elsewhere.[8]

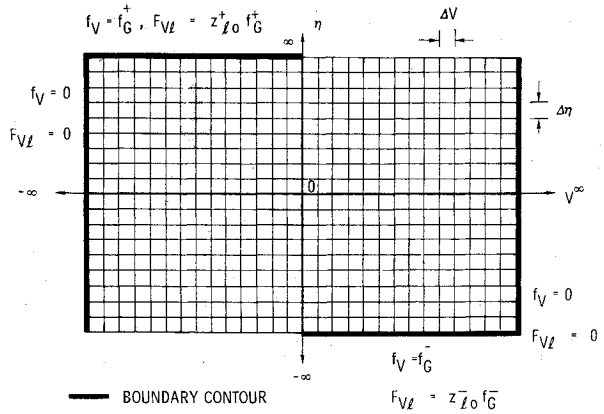

Fig. 2 Computational η-V domain.

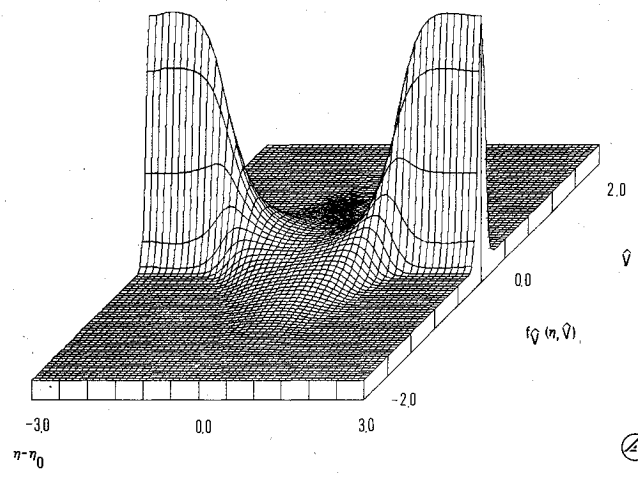

Fig. 3 Isometric plot of $f_{\hat{V}}$ over $(\eta, \hat{V})$ domain.

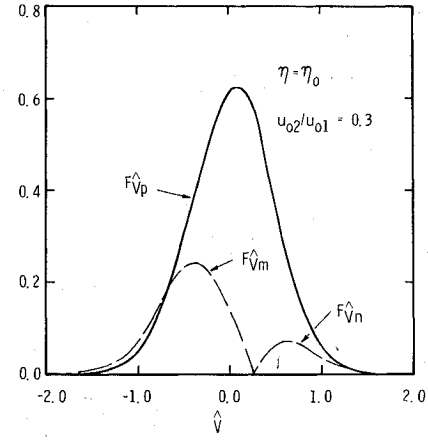

Fig. 4 Distributions of fuel (m), oxidant (n), and product (p) at $\eta=\eta_0$ for $u_{02}/u_{01}=0.3$.

The method of solution employed is a finite-difference scheme used to march in the x coordinate. The calculation is continued until the solution no longer changes with x. Central differencing is employed in the η and V coordinates, with the Dufort-Frankel[14] technique used to remove diffusion limitations on the allowable Δx step size. A leapfrog technique is used in x.

Discussion of Results

The present investigation extends previous work[8] that focused upon the fluid mechanical structure of the shear layer. The solution for the turbulence structure of the velocity

field, as discussed earlier, is included in the calculation of the diffusion flame as it is coupled to the species concentration field. However, detailed results and data comparisons will not be repeated here except to show a typical solution for $f_{\hat{V}}$ in Fig. 3 and briefly discuss its behavior. Figure 3 shows the evolution of $f_{\hat{V}}$ as the shear layer is traversed. Because the turbulence level is taken as small and equal in the two streams, $f_{\hat{V}}$ assumes the Gaussian form with high peak and narrow spread (low variance or turbulence energy) at the positive and negative extremes of η. Recall that the collapse of $f_{\hat{V}}$ to a delta function implies a zero turbulence energy or laminar flow at the mean velocity that becomes coincident with the instantaneous velocity. As the solution recedes from either boundary, two changes occur in the form of $f_{\hat{V}}$. First, a spreading occurs accompanied by a lowered peak. The result is a higher turbulence energy toward the interior of the shear layer, which agrees with observation. The other important characteristic of $f_{\hat{V}}$ is the skewing with respect to the $\hat{V}=0$ plane. The skewed pdf possesses nonzero odd-ordered moments that represent transport in the mean. The skewness is opposite in sense on either side of the dividing streamline representing the antisymmetric transport character of the shear layer. The structure of the transverse turbulence velocity field, as given by the solution for $f_{\hat{V}}$ just discussed, provides the framework for the fundamental chemical coupling responsible for the turbulent diffusion flame structure. This will be apparent in the subsequent discussion of the solutions obtained for the species distributions.

Figure 4 contains plots of the solutions for $F_{\hat{V}m}$ and $F_{\hat{V}n}$ for a specific value of η. The value 0.5 was chosen for the ratios $(a\hat{M}_r/d\hat{M}_p)$ and $(b\hat{M}_s/d\hat{M}_p)$. The numerical values for the boundary conditions are: $m_0^+=1.98$, $n_0^+=0$, $h_0^+=0.5$, $c_0^+=0.01$, and $m_0^-=0$, $n_0^-=1.4$, $h_0^-=0.5$, $c_0^-=0.3$. The manner in which the solutions satisfy Eq. (21) imposed by the fast reaction kinetics is clear from this figure. Nowhere are $F_{\hat{V}m}$ and $F_{\hat{V}n}$ simultaneously nonzero. A distinct location exists at which the two distributions are both zero and have discontinuous derivatives in $\hat{V}$ reminiscent of the well-known spatial profiles[11] of reactants for a laminar flame sheet. The difference is, of course, that it is the velocity space structure that is being observed.

A certain conceptual analogy does exist between the laminar flame sheet and the structure of the solutions shown in Fig. 4. The laminar flame sheet results from molecular transport across the adjacent diffusion layers to a point at which the reactants are brought into contact and can react. Because the mixing is a molecular process, the reactants are, by definition, "molecularly mixed" wherever they exist in the flame zone. The combustion reactions therefore proceed throughout a flame zone region that is of molecular dimensions resulting in, on a continuum level, an infinitely thin flame. In the present situation, transfer occurs through velocity space. Only when the reactants are brought into coexistence by the history of velocity fluctuations experienced by each reactant does the combustion proceed. Turbulent transport through physical space is viewed in the mean as an integral over velocity space and occurs on a much larger scale than molecular transport. However, the molecularly mixed state and fast-reaction interface occur at a distinct location in velocity space. As is evident in Fig. 4, much of each reactant is distributed throughout velocity space and is not molecularly mixed. As a result, when the reactant distributions are integrated over V, it is found that, even with infinite reactions, the reactants can coexist in the mean at a given value of η. As seen in Figs. 5-9, the extent of the region over which these conditions prevail is related to the turbulent length scale. The behavior of the solutions, as discussed herein, provides an explanation for the commonly referred to phenomenon in which reactants can be mixed turbulently on a large scale but cannot react until interdiffusion between large-scale structures completes the molecular mixing.

The three-dimensional plots of $F_{\hat{V}m}$ and $F_{\hat{V}n}$ are displayed in Figs. 5 and 6. The locus of points at which the reaction

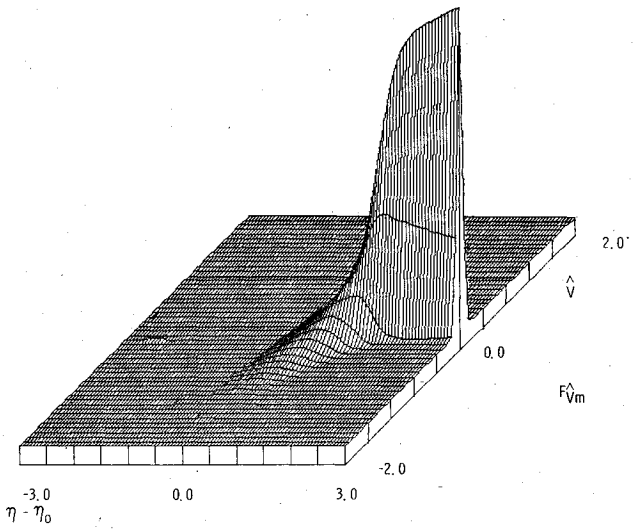

Fig. 5 Isometric plot of $F_{\hat{V}m}$.

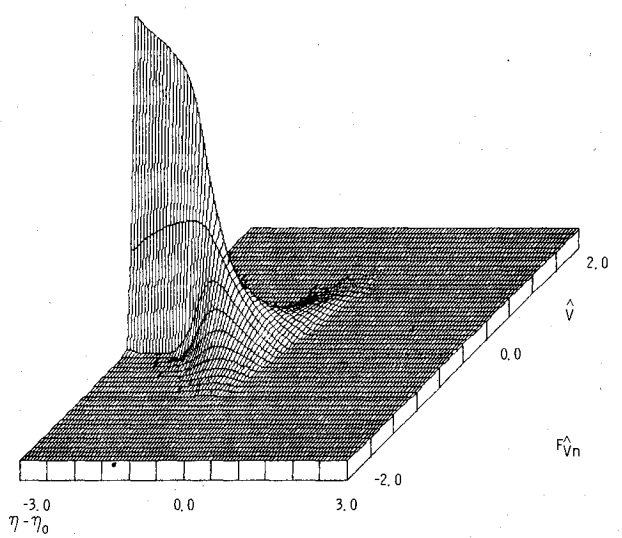

Fig. 6 Isometric plot of $F_{\hat{V}n}$.

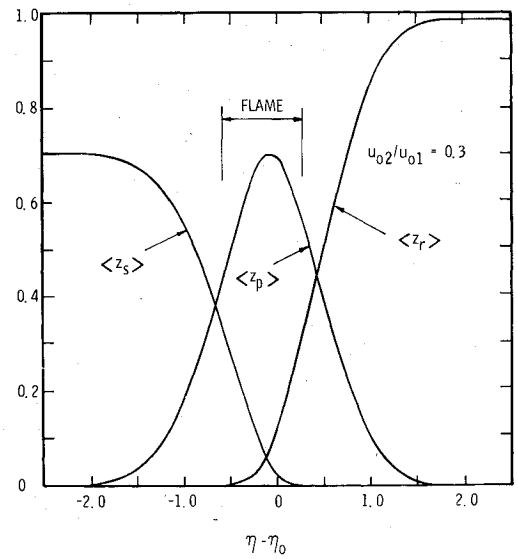

Fig. 7 Averaged species profiles of fuel (r), oxidant (s), and combustion product (p), $u_{02}/u_{01}=0.3$.

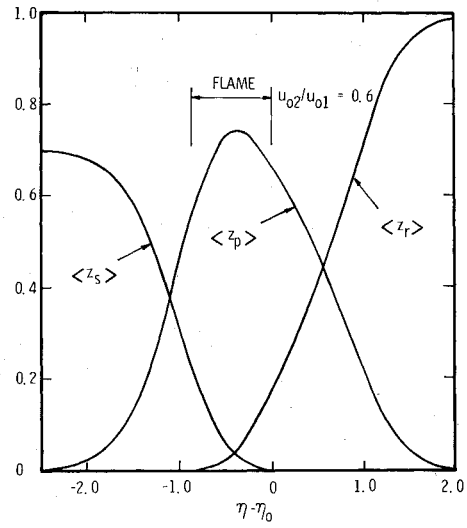

Fig. 8 Averaged species profiles for fuel (r), oxidant (s), and combustion product (p), $u_{02}/u_{01} = 0.6$.

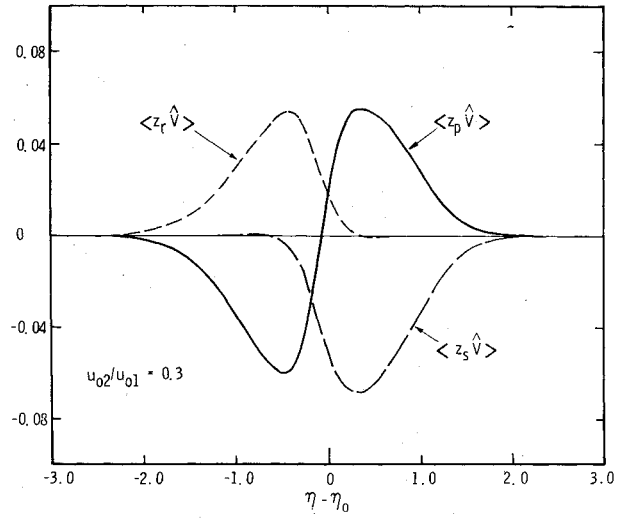

Fig. 9 Averaged transport profiles for fuel (r), oxidant (s), and combustion product (p), $u_{02}/u_{01} = 0.3$.

kinetics drive the reactant distributions to zero is clearly visible in Fig. 6. The fact that this line is not parallel to the $\hat{V}$ axis gives additional perspective to the explanation of how mean reactant profiles can overlap in the flame zone.

If this intersecting line between the solution and η-$\hat{V}$ plane were to rotate as a result of some parametric variation in the solution and become aligned with the $\hat{V}$ coordinate, the flame zone in physical space would collapse to a sheet. The solution would then resemble the laminar flame sheet solution with perhaps some augmented scalar transport coefficient. It is instructive to determine under what conditions this might happen. Inspection of Eqs. (3) and (4) reveals that, if the turbulent dissipation or interdiffusion rate βD goes to infinity, the velocity pdf becomes a delta function with the reactants uniformly distributed over velocity space. Physically this means that the reactants immediately become molecularly mixed as they are transported by the large-scale motions. However, the collapse of the velocity pdf to delta function implies the turbulence is damped. The conclusion is that, for a thin flame sheet to exist, there must be a simultaneous extinction of the turbulence or, in effect, laminar combustion. Figures 5 and 6 illustrate that if the solution were to drive toward a delta function, the intersecting line in the η-$\hat{V}$ plane would shrink to a point. The flame zone, whose extent is given by the projection of that line on the η axis, would also collapse to a sheet.

Having discussed the structure of the turbulent diffusion flame based upon the reactant distributions in velocity space, it remains to provide the mean structure by integrating the distributions over all $\hat{V}$. The results are plotted vs η in Figs. 7 and 8. As expected, the mean profiles of fuel and oxidizer overlap. The combustion product is formed in this overlap region defined as the flame zone and diffuses away. Note that the mean profiles are free from the discontinuous slopes associated with earlier approximate solutions to the present theory.[5] However, the fundamental nature of the solutions remains unchanged, confirming that the thickness of the turbulent flame zone is of the order of the turbulent length scale.

This becomes apparent when the flame thickness, denoted by η_f, is transformed to δ_f in physical space by means of Eq. (17) and compared with $\Lambda = \ell_s x$ with the following result:

$$\delta_f/\Lambda = \eta_f/\sigma\ell_s \tag{25}$$

Inspection of Figs. 7 and 8 shows η_f to be ≈ 0.8, whereas $\sigma\ell_s$ is 0.88 and 0.8 for $r = 0.3$ and 0.6, respectively. The result is that δ_f/Λ is 0(1). This result shows that the scaling of the flame zone with turbulence length scale is insensitive to overall shear between the two streams.

The turbulent transport profiles for the fuel (r), oxidant (s), and combustion product (p) vs η are shown in Fig. 9. These are obtained by multiplying $F_{\hat{V}r}$, $F_{\hat{V}s}$, and $F_{\hat{V}p}$ by $\hat{V}$ and integrating over all $\hat{V}$ and are therefore a product of the solutions. The transport in the mean results from the statistical nonequilibrium of the distributions. The statistical nonequilibrium of $f_{\hat{V}}$ shown in Fig. 3 is driven by the velocity shear between the two streams, whereas that of the species distributions apparent in Figs. 5 and 6 couples in the effects of the reactions.

Concluding Remarks

Numerical solutions in velocity space of the turbulent diffusion flame have been obtained for the first time based upon the kinetic theory of turbulence presented in this paper. The treatment is based upon the transverse component of the turbulence velocity field that governs the turbulent transport phenomena in the two-dimensional shear layer. The solutions consist of the pdf of the velocity field as well as the species distributions.

The solutions for the reactant distributions display a curious structure in velocity space. Because of the enforcement of infinite reaction rates at each point of velocity space, a distinctive line exists in the η-$\hat{V}$ plane at which $F_{\hat{V}m}$ and $F_{\hat{V}n}$ are simultaneously zero and have discontinuous slopes. This appearance is reminiscent of a flame sheet; however, close inspection of the solution shows exactly the opposite. In fact, examination of the solution provides an explanation for the existence of thick, turbulent diffusion flames which states that reactions between turbulently mixed reactants cannot proceed until molecular mixing occurs. The governing mechanism within the model for this physical phenomenon is that the species are carried by the fluid elements whose turbulence velocity field is given by the pdf for $\hat{V}$. Therefore, the species are considered to be intimately in contact or molecularly mixed only when they occupy the same cell in velocity space.

The final result of the calculations is obtained by integrating the distributions over velocity space to obtain mean reactant profiles in the shear layer. These profiles define a thick, turbulent flame in which oxidizer and reactant coexist in the *mean*.

The present results, which extend the work of Ref. 8, further substantiate the utility of direct numerical solutions of the governing equations for the kinetic theory of turbulence presented here. The direct numerical solutions remove certain manifestations of the previously employed approximate methods, such as discontinuous slopes in the mean profiles.

They also foster deeper insight into the important physical phenomena through their more detailed structure. Finally, such calculations extend the applicability of the KTT to practical engineering geometries.

Acknowledgments

The author wishes to acknowledge the many useful discussions held with Dean P. M. Chung of the University of Illinois, Chicago, and Dr. T. C. Lin of TRW.

References

[1] Rhodes, R. P., Harsha, P. T., and Peters, C. E., "Turbulent Kinetic Energy Analysis of Hydrogen-Air Diffusion Flows," *Acta Astronautica*, Vol. 1, 1974, pp. 443-470.

[2] Alber, I. E. and Batt, R.G., "Diffusion-Limited Chemical Reactions in a Turbulence Shear Layer," *AIAA Journal*, Vol. 14, Jan. 1976, pp. 70-76.

[3] Chung, P. M., "Turbulent Chemically Reacting Flows," The Aerospace Corp., El Segundo, Calif., Tech. Rept. TR-1001 (S2855-20)-5, 1967.

[4] Chung, P. M., "A Simplified Statistical Model of Turbulent Chemically Reacting Shear Flows," *AIAA Journal*, Vol. 7, Oct. 1969, p. 1982.

[5] Chung, P. M., "Diffusion Flame in Homologous Turbulent Shear Flows," *Physic of Fluids*, Vol. 15, Oct. 1972a, p. 1735-1749.

[6] Chung, P. M., "A Kinetic-Theory Approach to Turbulent Chemically Reacting Flows," *Combustion Science and Technology*, Vol. 13, 1976, pp. 123-153.

[7] Liu, C. Y. and Lees, L., "Kinetic Theory Description of Plane Compressible Couette Flow," *Rarefied Gas Dynamics*, edited by L. Talbot, Academic Press, N.Y., 1961, pp. 391-428.

[8] Bywater, R. J., "A Velocity Space Description of Certain Turbulent Free Shear Flow Characteristics," *AIAA Journal*, Vol. 19, Aug. 1981, pp. 969-975.

[9] Janicka, J., Wokolbe, W., and Kollmann, W., "The Solution of a PDF-Transport Equation for Turbulent Diffusion Flames," *Proceedings of the 1978 Heat Transfer and Fluid Mechanics Institute*, Stanford University Press, 1978.

[10] Chung, P. M., "Turbulence Description of Couette Flow," *Physics of Fluids*, Vol. 16, July 1973, p. 880.

[11] Williams, F. A., *Combustion Theory*, Addison-Wesley, London, 1965.

[12] Spencer, B. W. and Jones, B. G., "Statistical Investigation of Pressure and Velocity Fields in the Turbulent Two-Stream Mixing Layer," AIAA Paper 71-613, 1971.

[13] Schlichting, H., *Boundary Layer Theory*, McGraw-Hill Book Co., New York, N.Y., 1955.

[14] Roache, P. J., *Computational Fluid Dynamics*, Hermosa Publishers, Albuquerque, N. Mex., 1972.